

Exchange-excited f - f transitions in the electron-energy-loss spectra of rare-earth metals

F. Della Valle and S. Modesti

*Dipartimento di Fisica, Università degli Studi di Trieste, via A. Valerio 2, I-34127 Trieste, Italy
and Laboratorio Tecnologie Avanzate Superfici e Catalisi del Consorzio Interuniversitario Nazionale
per la Fisica della Materia, Padriciano 99, I-34012 Trieste, Italy*

(Received 27 July 1988; revised manuscript received 15 March 1989)

Dipole-forbidden f - f multiplet excitations are found to characterize the electron-energy-loss spectra of Pr, Nd, Sm, Gd, Tb, Dy, Ho, and Er when the primary-electron energy is close to the binding energy of the $4d$ electrons. In Sm and Gd the f - f transitions are also detected at lower primary energies. The identification of the sharp peaks observed in the spectra as f - f excitations comes from straightforward comparison with the absorption spectra of the trivalent ions. The excitation energies of the f - f transitions are found to depend very weakly on the chemical environment. The exchange nature of the f - f excitation process explains the strong decrease of the intensities of the f - f peaks when the primary energy is raised, and is consistent with the resonant enhancement observed for primary energies near the $4d$ - $4f$ threshold. A similar resonance is also observed in the primary-energy dependence of the intensity of the plasmon peak.

I. INTRODUCTION

Dipole-forbidden electronic transitions, in particular, spin-forbidden transitions, have been observed and studied in atoms¹ and molecules² by electron-energy-loss spectroscopy (EELS) for a long time. In many cases it was natural to associate the excitation mechanism of these transitions with an exchange process, since their cross sections are strongly enhanced when the primary-electron energy E_p is close to the excitation energy and the scattering angle is large.^{1,2} In the exchange process, in contrast to the case of dipole scattering, the primary electron and the detected electron are different, the latter being an electron ejected from the sample when the former is captured into an empty state.

In the interpretation of reflection EEL spectra from solids, however, it has been customary for a long time to invoke exclusively dipole mechanisms, and to ignore exchange. Recently, clear evidence of dipole-forbidden exchange transitions has been observed in the inner-shell excitation EEL spectra of transition metals³ and metallic rare earths.⁴ The exchange mechanism has also been successfully used to explain the spin-polarized valence-band EEL spectra of Fe-B-Si alloys,⁵ Ni,⁶ Fe,⁷ and bcc Co (Ref. 8) in terms of majority spin to minority spin d -band transitions (Stoner excitations).⁹ Moreover, the strong primary-energy dependence of the excitation process has allowed the identification of Stoner excitations also in ordinary (not spin-polarized) EELS.^{10,11}

Data for the transition metals⁵⁻¹¹ show that EEL spectra of solids, taken in the reflection mode, contain contributions from exchange transitions whose intensity, for low E_p , can be comparable to that of ordinary dipole-allowed transitions. However, the identification of such transitions may not be easy if the involved bands have a large dispersion. In the rare-earth metals (REM's) Sm, Eu, Gd, Tb, Dy, Ho, and Er, in which the f levels retain

most of their atomic character, exchange excited f - f transitions give rise to the most pronounced and sharpest features in the EEL spectra taken at low E_p .^{12,13} In these cases, the excitation mechanism consists in the capture of the primary electron into an empty f state, and the ejection of another electron from the same f shell. Because of the sharpness of the f - f peaks it was relatively easy to study the intensity of these optically forbidden transitions as a function of E_p . A resonant enhancement was observed when E_p reaches the $4d$ - $4f$ core threshold, consistently with what is expected for an exchange excitation mechanism.¹²

In this work we report new data on metallic Sm, Gd, Tb, Dy, Ho, and Er, and extend the investigation to Pr, Nd, and Yb; f - f transitions are found in the EEL spectra of all the REM's with unfilled f levels. In all cases the results follow the same pattern, which can be summarized as follows: (a) the low-energy part of the EEL spectrum is characterized, for low E_p , by multiplets of f - f transitions; (b) these multiplets agree well with the weak lines observed in the optical-absorption spectra of the trivalent ion; (c) the structures in the spectrum of the metal with n f electrons can also be related to the shake-up features seen in the x-ray photoemission spectrum of the metal with $n+1$ f electrons and in the bremsstrahlung isochromat spectrum (BIS) of the metal with $n-1$ f electrons; (d) the localized nature of the states involved in the transitions is reflected in the small linewidths (40–100 meV) of the components of the multiplets and in their insensitivity to chemical bonding; (e) there is a resonant enhancement of the intensity of all the multiplets when the primary energy E_p reaches the $4d$ - $4f$ core excitation energy; and (f) the dipole-allowed plasmon peak is also resonantly enhanced.

II. EXPERIMENTAL PROCEDURE

The Gd and Dy samples were single crystals, while Pr, Nd, Sm, Tb, Ho, Er, and Yb were in polycrystalline form.

The samples were mechanically polished with diamond paste and immediately inserted in an ultrahigh-vacuum chamber with a fast-load system in order to minimize oxidation. Their surfaces were cleaned by Ar^+ sputtering until the coverage of the contaminants (mainly oxygen) was less than 0.02 monolayer, as estimated by Auger spectroscopy.¹⁴ The EEL spectra showed appreciable modifications when the oxygen coverage increased, as discussed below.

In the low resolution EELS measurements the primary-electron incidence angle was 60° , and the back-scattered electrons were collected in a 6° cone along the normal to the surface and analyzed by a hemispherical analyzer operated in the constant resolution mode, with an overall energy resolution of 0.5 eV—full width at half maximum (FWHM) of the elastic peak. The primary-electron energies, referred to the analyzer vacuum level, were measured with an accuracy of ~ 1 eV. Since the residual gas pressure in our system was $\sim 2 \times 10^{-8}$ Pa and the time required to complete a set of data for different E_p 's was a few hours, we sputtered the sample while measuring, to avoid excessive contamination. The cleanliness of the Sm sample was also checked by x-ray photoelectron spectroscopy (XPS), by measuring the intensity of the surface divalent component in the $3d$ photoemission spectrum.¹⁵

High-resolution EEL (HREEL) spectra of Dy were measured, using a commercial Leybold-Heraeus ELS 22 analyzer, in specular geometry, with an incidence angle of 60° . In order to obtain high count rates the resolution was limited to 15 meV. The sample was cleaned by Ar^+ sputtering and the spectra recorded within one hour after the cleaning process at a working pressure of 10^{-8} Pa. The primary energy was 20 eV.

Because of surface disorder due to the polishing and sputtering processes, and of the large collection angle for the low resolution measurements, all our spectra may be regarded as essentially momentum integrated.

III. RESULTS AND DISCUSSION

A. EEL spectra

Panels (a) and (e) in Figs. 1–4 show the reflection EEL spectra of metallic $\text{Pr}(f^2)$, $\text{Nd}(f^3)$, $\text{Sm}(f^5)$ configuration in the bulk and, at least partially, f^6 at the surface,^{15,16} $\text{Gd}(f^7)$, $\text{Tb}(f^8)$, $\text{Dy}(f^9)$, $\text{Ho}(f^{10})$, $\text{Er}(f^{11})$, and oxidized $\text{Yb}(f^{13})$ (Ref. 23) taken at different primary energies E_p . The top spectrum in each panel corresponds to a primary energy a few tens of electron volts lower than the $4d$ binding energy E_{4d} , while the other refer to E_p slightly higher than E_{4d} (second spectrum from the top) and much higher than E_{4d} . A marked E_p dependence is observed for all these metals, with the exception of Yb. In particular, the high E_p spectra closely resemble the published loss functions,^{19–22} showing a broad plasmon peak at 8–13 eV, and the EELS data of Netzer *et al.*²⁴ On the contrary, the low E_p spectra display sharp extra structures.

Panels (b) and (f) in Figs. 1–4 show energies and intensities of the very faint absorption lines observed in the

optical-absorption spectra of the trivalent ions in solution. These lines are due to f - f transitions very weakly allowed in an environment without inversion symmetry (a typical oscillator strength is $\sim 10^{-6}$).¹⁷ An f - f transition can take place either with or without a spin flip of the excited electron. In the case of an f^7 configuration (Eu and Gd) all the f - f transitions involve spin flip.

Where possible [panels (c) and (g)] the EEL spectra of the REM with n f electrons are compared with the published BIS of the metal with $n-1$ f electrons or with the x-ray photoemission spectrum of the metal with $n+1$ f electrons.¹⁸ The reason for doing this is that, when an extra electron is added to an atom with $n-1$ f electrons by an inverse photoemission process, the system is left either in the ground or in the excited states of the f^n

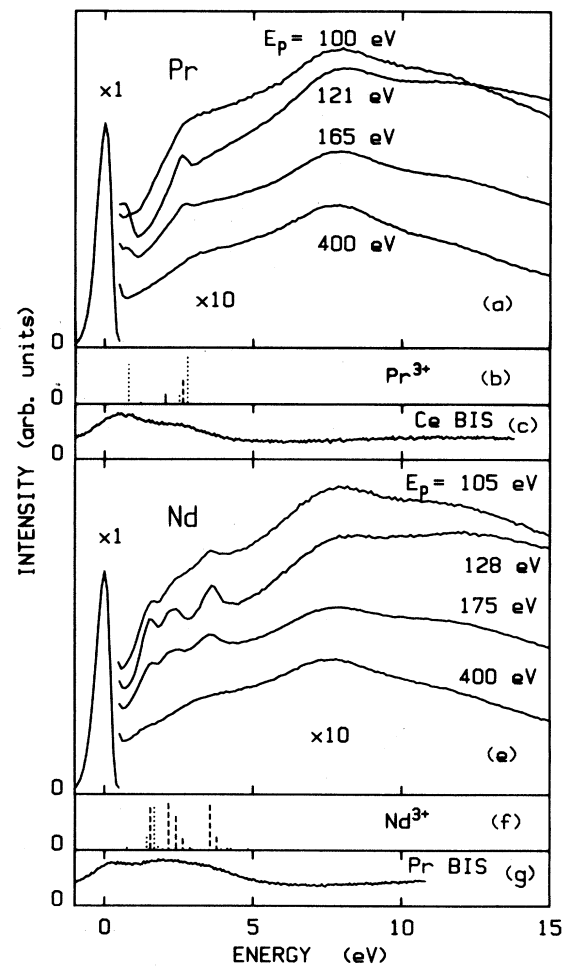


FIG. 1. Energy-loss spectra of (a) Pr and (e) Nd for the indicated primary energies E_p . Optical-absorption spectra of (b) Pr^{3+} and (f) Nd^{3+} from Ref. 17 showing the f - f transitions; solid lines correspond to transitions involving spin flip, dotted lines indicate nonflip transitions, and dashed lines represent the overlap of both flip and nonflip transitions. BIS of (c) Ce and (g) Pr from Ref. 18 (see text). The scale in the abscissa refers to energy loss ω for (a) and (e), to photon energy for (b) and (f), and to kinetic energy for (c) and (g) (see text).

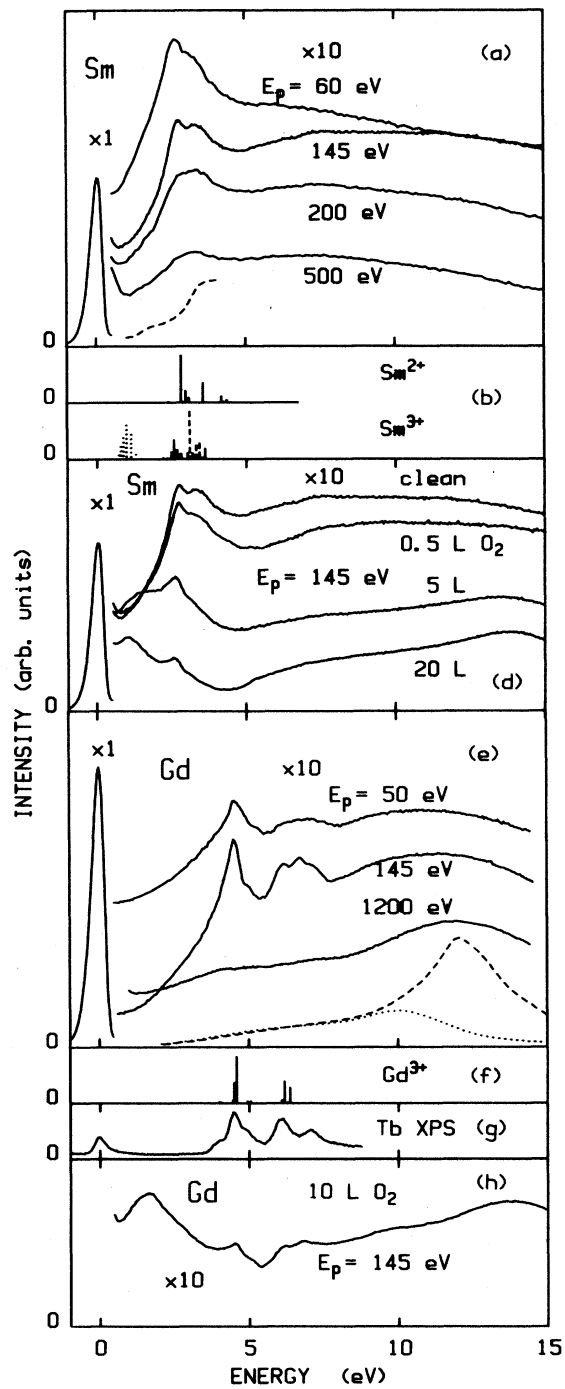


FIG. 2. Same as Fig. 1, but for Sm and Gd. Dashed and dotted lines in (a) and (e) show bulk and surface loss functions, respectively, taken from Refs. 19 (Sm) and 20 (Gd). The energies of the f^6 excitations of Sm^{2+} in (b) have been obtained by a 10% contraction of the spectrum of the Eu^{3+} ion. (g) shows the x-ray photoemission spectrum of Tb from Ref. 18 (see text). (d) and (h) show the EEL spectra of oxidized Sm and Gd, respectively [1 langmuir (L) $\equiv 10^{-6}$ torr s]. Energy scale in (d) and (h) as for (a) and (e). For the sake of clarity the spectrum at $E_p = 50$ eV in (e) has been shifted upward by 20% of the height of the window.

configuration. These states show up as distinct features in the BIS.¹⁸ The f - f multiplets observed in the EEL spectra of the f^n metal and those observed in the BIS of the f^{n-1} metal should therefore be very similar, the main difference being the energy scale, which in the latter case is contracted by $\sim 10\%$ with respect to the former one because of the smaller atomic number Z .¹⁸ A similar line of reasoning holds for the comparison of the EEL spectra of the f^n metal with the x-ray photoemission spectrum of the metal with $n+1$ f electrons, with the obvious difference that the energy scale is now expanded by about the same amount.^{25,18} In both cases (BIS or XPS), the energy zero corresponds to the energy of the ground state of the f^n configuration.

On the basis of the comparison with the optical, photoemission, and inverse photoemission spectra, it has been possible to identify the transitions that give rise to peaks in the EEL spectra. Table I summarizes this information by giving the quantum numbers S , L , and J of the states involved.

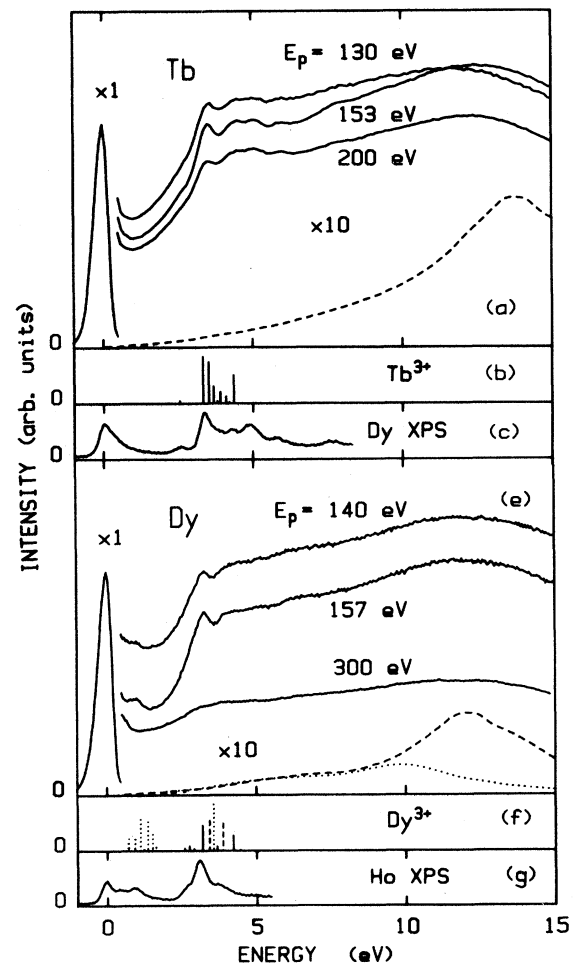


FIG. 3. Same as Figs. 1 and 2, but for Tb and Dy. Loss functions from Ref. 21 (Tb) and Refs. 20 and 22 (Dy). The spectrum at $E_p = 157$ eV in (e) has been shifted downward by 10% of the height of the window.

The energies of the first peak of the BIS of Ce and Pr [Figs. 1(c) and 1(g)] appear to be slightly higher than zero because of the contributions from several excited states [3H and 3F for Pr,²⁷ and 4I for Nd (Ref. 28)]. The peak at $\omega \approx 0.8$ eV in the Pr EEL spectra (mainly attributable to 3F states) is not clearly resolved because of the experimental resolution of 0.5 eV and the presence of excited 3H_J states up to 0.6 eV.^{27,29}

In contrast to Pr and Nd, in Sm and Gd the f - f transitions are strong also in the spectra taken with $E_p < E_{4d}$. The contribution from divalent and trivalent Sm overlap in the region 2–4 eV, making it difficult to evaluate their relative importance in the EEL spectra. The 6F transitions of the trivalent f^5 configuration expected at $\omega \sim 1$ eV are not observed in the clean sample, and may be masked by the tail of the elastic peak. The Sm sample

TABLE I. Labeling of the f - f transitions observed in the EEL spectra of REM's. Second and fourth columns give the quantum numbers S , L , and J for the initial and final states, respectively. Excitations of Sm^{2+} have been identified with f - f transitions of Eu^{3+} .

Element	$^{2S+1}L_J$	ω (eV)	$^{2S'+1}L'_J$	References
Pr f^2	3H_4	0.8	3F	17,26
		2.6	3P	17
Nd f^3	$^4I_{9/2}$	1.6	4F	17,26
		2.3	4G	17
		3.7	$^4D, ^2L, ^2I$	17
Sm f^5	$^6H_{5/2}$	1.0	6F	17,26
		2.7	$^4F_{5/2}$	17,26
		3.3	6P	17,26
Sm f^6	7F_0	2.7	$^5L_6, ^5G$	17
		3.3	5H_6	17
Gd f^7	$^8S_{7/2}$	4.5	6I	17,25,26
		5.0	6D	17,25,26
		6.2	6G	17,25,26
		6.7	6F	25,26
		7.2	6H	25,26
Tb f^8	7F_6	2.6	5D_4	17,25,26
		3.6	$^5G, ^5L$	17,25,26
		4.4	$^5I, ^5F$	17,25,26
		5.2	$^5G, ^5K$	25,26
		6.1	5H	26
8.0	$^5I, ^5F$	26		
Dy f^9	$^6H_{15/2}$	1.0	$^6H, ^6F$	17,25,26
		3.3	$^4I, ^4M_{21/2}, ^4M_{19/2}, ^4K_{17/2}$	17,25,26
		3.9	$^4G, ^4L, ^4M_{17/2}, ^4K_{15/2}, ^4L_{19/2}$	17,25,26
		4.3	$^4H_{13/2}, ^4H_{11/2}, ^4K_{13/2}, ^4G$	17,26
		5.2	4I	26
		6.3	$^4H, ^4G$	26
Ho f^{10}	5I_8	0.7	5I_7	25,26
		2.8	$^5G, ^3K$	17,25,26
		3.6	$^5G, ^3G, ^3H, ^3L_9$	17,25,26
		4.4	$^3M_{10}, ^1L_8, ^5G_4$	17,25,26
		7.0	3K	26
Er f^{11}	$^4I_{15/2}$	0.8	$^4I_{13/2}$	17,25,26
		1.4	$^4I_{11/2}, ^4I_{9/2}$	17,26
		2.4	$^2H_{11/2}, ^4F_{7/2}$	17,25,26
		3.4	$^2K_{15/2}, ^4G_{11/2}, ^4G_{9/2}, ^4G_{7/2}$	17,25,26
		5.1	$^2L, ^4D, ^2I$	17,25,26
Yb f^{13}	$^3F_{7/2}$	1.3	$^2F_{5/2}$	17,25

has been deliberately oxidized in order to follow the spectral change during oxygen chemisorption. The reason for doing this is that oxygen completely removes the f^6 configuration for exposures higher than 10 langmuir (L).³⁰ While oxygen chemisorption shifts the broad plasmon peak and gives rise to a new structure at $\omega=1$ eV, it only shifts down the f - f peak at $\omega=2.7$ eV by 0.1 eV. This shift might be due to the modified weight of the

f^5 and f^6 contributions in the 2.7-eV peak. The new structure at $\omega=1$ eV can be attributed to 6F excited states of the f^5 configuration. It should be noted incidentally, that the dependence of the spectra on the oxygen exposure rules out the possibility that the sharp peaks observed in Sm could be related to residual oxygen contamination. The spectra of oxidized Gd, already discussed in Ref. 12, show a behavior similar to the Sm case. In particular, the f - f transitions are only affected in their intensities. Both in the clean and oxidized surfaces these transitions occur at the same energies within the limit of our experimental accuracy, as expected from the strong localization of the f levels.

The f - f peaks in the EEL spectra of Tb, Dy, Ho, and Er are weaker than in Sm and Gd. This finding is consistent with the expectation of an f - f excitation probability that is proportional to the product of the number of f electrons (n) times the number of empty f states ($14-n$), which has its maximum at $n=7$. Moreover, most of the peaks fall within an energy range (3–5 eV) where the surface loss function $\text{Im}[-1/(\epsilon+1)]$ has a maximum.^{20,22} In addition, dipole-allowed single-particle excitations contribute to the spectrum in this energy range.³¹ The bump at $\omega=4.4$ eV in Er does not correspond to any strong f - f transition in the Er^{3+} ion,^{17,25,26} but coincides with a broad maximum of the surface loss function.²²

In contrast to all the other REM's discussed so far, no low-energy sharp structures are present in the case of metallic Yb, as expected from its complete f -shell configuration (f^{14}). The spectra we measured are in perfect agreement with those by Onsgaard and Chorkendorff³¹ and Bertel *et al.*,³² and are therefore not reported here. The spectra are characterized by two broad peaks, the first at $\omega=4.3$ eV, due to the surface plasmon³³ with substantial contribution from dipole interband transitions^{31,34} and the second one at $\omega=9$ eV, the bulk plasmon loss.³³ An f - f transition at 1.28 eV is expected to be present in the case of the f^{23} configuration of Yb^{3+} .^{17,25} This configuration can be obtained by oxidizing the clean metal.²³ We therefore exposed the Yb surface to oxygen, until a strong $4d$ - $4f$ threshold appeared in the EEL spectra at energy loss $\omega=182$ eV, pointing to the presence of empty f states.³² The EEL spectrum of Yb after this treatment (40 L oxygen exposure) is shown in Fig. 4(h). The spectrum is in fair agreement with those reported by Bertel *et al.*³² as far as the high-energy-loss region is concerned, but shows a double peak in the low-energy-loss region. The first structure falls at 1.3 eV, in good agreement with what is expected for the f - f transition,^{17,25} whereas the higher-energy peak, at 2.5 eV, is unexplained.

The EEL spectrum of Eu has been measured by Bauer and Kolackiewicz¹³ at low primary energy. A sharp peak is present in their spectrum at $\omega=3.9$ eV. This feature must have the same nature (${}^8S_{7/2} \rightarrow {}^6I$ transitions) as the strong peak at $\omega=4.5$ eV in the Gd spectrum, since the two metals have the same f^7 configuration. The 12% difference in energy between the two is again accounted for by the difference in nuclear charge.

A broad peak at $\omega=4.5$ eV has been observed in Tm by Onsgaard *et al.*³⁵ We argue that this feature contains

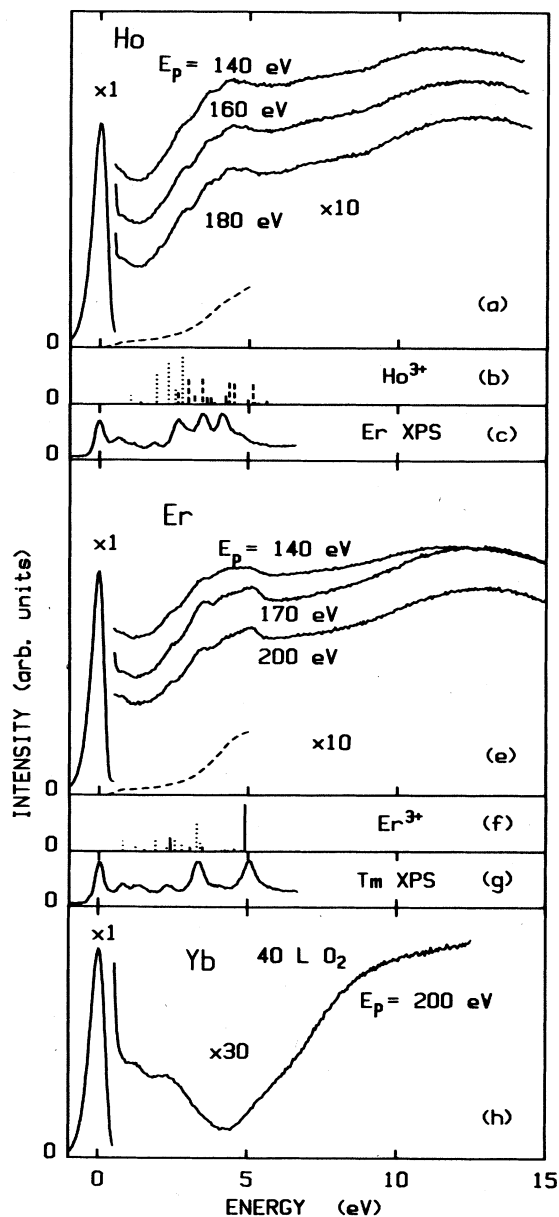


FIG. 4. Same as Figs. 1 and 2, but for Ho and Er. Loss functions from Ref. 22. (h) shows the EEL spectrum of oxidized Yb. The spectra at $E_p=140$ eV and $E_p=180$ eV in (a) have been shifted by 10% of the height of the window upward and downward, respectively. The spectrum at $E_p=140$ eV in (e) has been shifted upward by 10% of the height of the window.

contributions from f - f excitations. In fact, the absorption spectrum of Tm^{3+} is characterized by strong lines between 4 and 5 eV.^{17,26} Moreover, the BIS of $\text{Er}(f^{11})$ shows a broad bump at an energy ~ 4 eV higher than the position of the 3H_6 state (ground state of the f_{12} configuration of Tm).¹⁸

B. Intrinsic width and chemical shifts of the f - f transitions

In order to study the intrinsic linewidth of the f - f transitions and their energy shifts in the ionic, metallic, and oxidized states, we measured the loss spectrum of Dy a second time using a HREELS apparatus with an energy resolution of 15 meV. As shown in Fig. 5, the peak of Dy at $\omega=1$ eV is now resolved in its components, a strong line at 0.44 eV (FWHM 40 meV) and three weaker and broader structures at 0.73, 0.96, and 1.12 eV (FWHM) ~ 100 meV). The energies of the first three peaks coincide within 10 meV with those of the f - f transitions in the Dy ion.³⁶

Heavy oxidation (3000 L oxygen exposure) shifts the structures by a few tens of millielectron volts towards higher energies. The very small linewidth and sensitivity to the environment of these transitions are consistent with the localized nature of both the initial and final states involved, and point to a common energy dependence of both states on the chemical bonding. These results are in agreement with the data of Bauer and Kolaczkiwicz on Eu, Gd, and Tb.¹³ These authors observe no difference in the f - f peaks appearing in the EEL spectra of atomically dispersed and single-crystal rare earths.

C. Resonant enhancement of the EEL spectra

Figures 6–9 show the intensity of the plasmon peak and of some of the f - f peaks as a function of the primary-electron energy E_p . The intensities have been normalized to the height of the elastic peak, and no back-

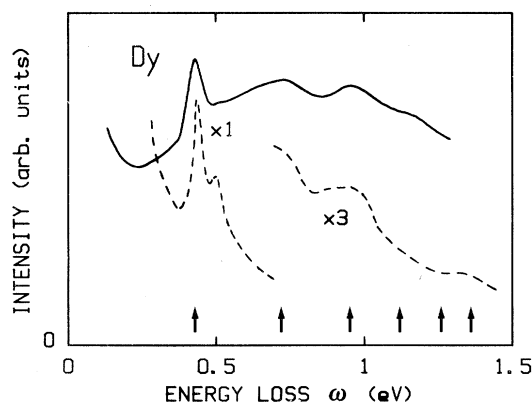


FIG. 5. High resolution EEL spectra of clean Dy (solid line) and oxidized Dy (dashed line). The oxygen exposure was 3×10^3 L. Primary energy was 20 eV, and energy resolution was 15 meV. The arrows show the energies of the f - f transitions in Dy^{3+} (Ref. 36).

ground subtraction has been attempted. The solid line at the bottom of each figure is the $4d \rightarrow 4f$ absorption threshold measured by EELS with $E_p \approx 2000$ eV. If we assume that the dominant contribution in the spectra comes from a two-step scattering process (elastic diffraction preceded or followed by inelastic scattering), as in the dipole-scattering case,³⁷ the normalized data should grossly mimic the primary-energy dependence of the f - f excitation cross sections, geometric and diffraction effects being largely canceled by the normalization to the intensity of the elastic peak.

The common characteristic of all the intensity versus E_p curves is the clear enhancement observed when E_p is close to the $4d$ binding energy, in correspondence with the onset of the $4d \rightarrow 4f$ threshold. Note that different excitations in the same metal have a different dependence on E_p . This result rules out the possibility that the observed enhancement is an artifact due to the attenuation of the elastic peak when a $4d$ hole is created. In Fig. 9 the E_p dependence of the 4.5-eV peak of Er is also shown. This structure, containing contributions from the surface plasmon as well as interband transitions, shows a much weaker jump. In this case, the weak resonance can be attributed to an enhancement of a background of multiple losses which involve f - f transitions.

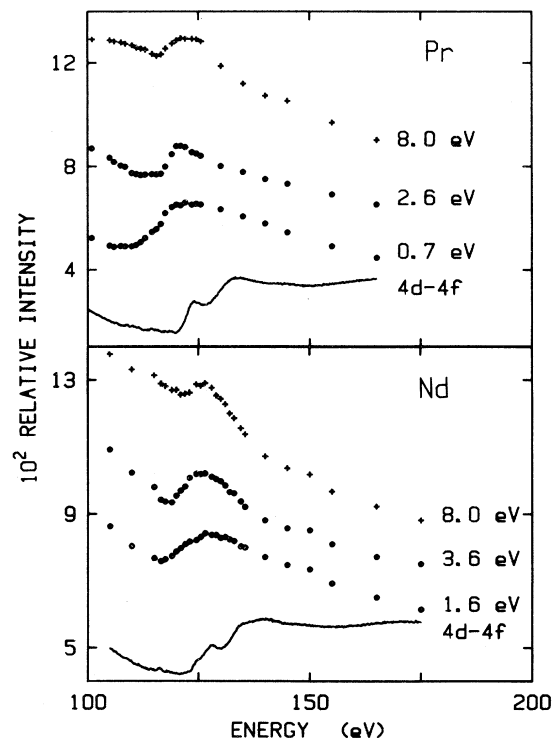


FIG. 6. Normalized intensities of the plasmon peak (crosses) and of some f - f peaks (dots) in the loss spectra of Pr and Nd plotted as functions of the primary-electron energy. The energies of the peaks are indicated in the figures. The solid lines show the EEL spectra of the $4d \rightarrow 4f$ core threshold measured with $E_p = 2000$ eV. In this latter case the energy scale refers to energy loss ω .

losses which involve f - f transitions.

As already discussed in Ref. 12, a new exchange collision channel opens when E_p reaches the $4d$ - $4f$ excitation threshold. In the new process [sketched in Fig. 10(b)] the energy lost by the primary electron falling into an f -state (f_1) excites a $4d$ electron into another $4f$ state (f_3) ($4d^{10}4f^n + e^- \rightarrow 4d^9 4f^{n+2}$). The intermediate $4d^9 4f^{n+2}$ state decays, via a super Coster-Kronig transition, into a $4d^{10}4f^n$ excited state (excitation energy ω) plus an outgoing electron at energy $E_p - \omega$. This same final state can also be reached by a normal exchange excitation of the f - f transitions [Fig. 10(a)]. Therefore, the two processes can interfere constructively, giving rise to the observed behavior of the intensities of the f - f peaks when E_p reaches E_{4d} .¹² This mechanism is analogous to that of resonant photoemission. In the EELS case, however, the intermediate state contains two extra f electrons instead of one. This intermediate state cannot be reached in oxidized Yb, which has thirteen electrons in the f shell. Therefore, the loss peak at 1.3 eV in this system should not resonate. Our measurements confirm this expectation within the experimental accuracy.

The $4d$ - $4f$ optical thresholds are characterized by several sharp lines followed by a broader peak at an energy ~ 10 eV higher.³⁸ The sharp lines are very weak in Sm and Gd, and grow in intensity in the heavier elements (Dy, Ho, Er), where they become more and more optically allowed.³⁹ The sharp jump in the f - f cross section in

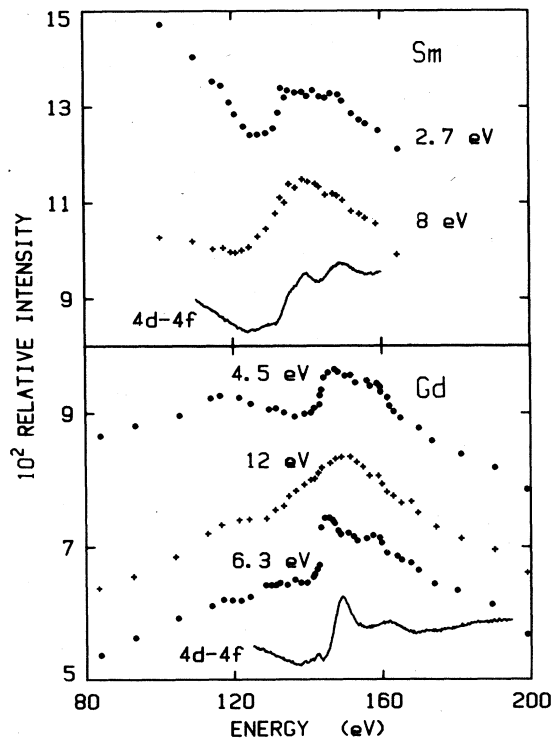


FIG. 7. Same as Fig. 6 but for Sm and Gd. For the sake of clarity the intensity curve of the 4.5-eV loss of Gd has been shifted upward by 1 unit.

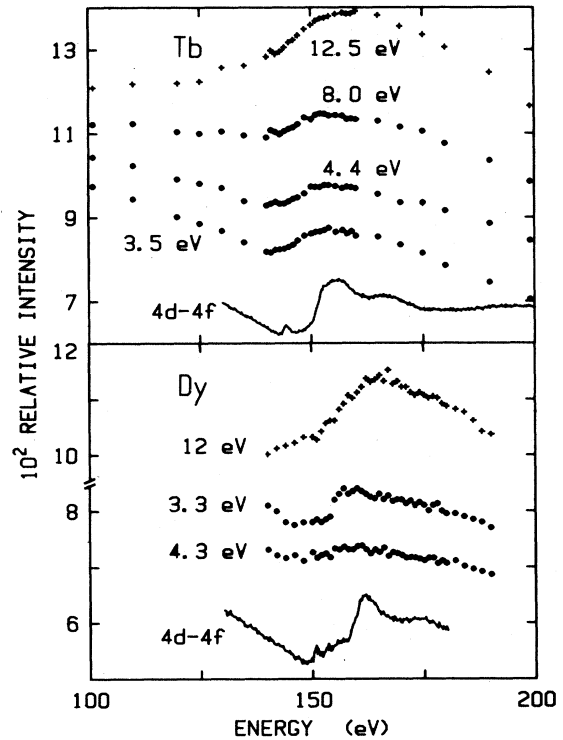


FIG. 8. Same as Fig. 6 but for Tb and Dy. The intensity curve for the Tb plasmon (labeled 12.5 eV) has been shifted by 3 units upward, the 8-eV curve by 2 units, and the 4.4-eV curve by 1 unit.

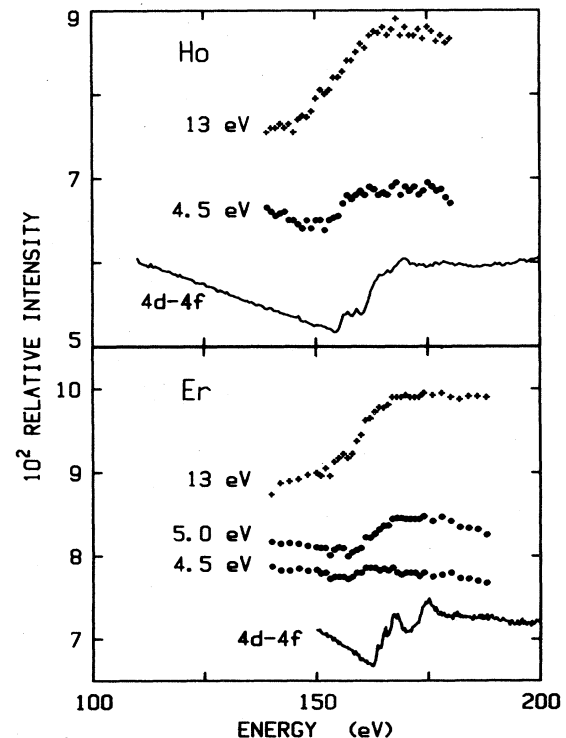


FIG. 9. Same as Fig. 6 but for Ho and Er.

Nd, Pr, Sm, and Gd occurs at an energy E' which corresponds to the edge of the broad and strong optical-absorption peak. In the heavier rare earths the energy E' gets closer to that of the sharp absorption lines. In other words, there is an enhancement in the intensity of the exchange excited transitions related to the dipole cross section of the $4d$ - $4f$ core excitation. This finding is in agreement with the proposed resonance mechanism.

As far as the core-level-related enhancement of the dipole-allowed plasmon excitation is concerned, we note that in Pr and Nd the resonance is weaker than in the other metals, and has a shape similar to that of the resonance of the f - f transitions. Since each point of the spectra shows similar behavior in intensity, as a function of E_p , the effect could be attributed to a background of multiple losses that involve f - f transitions. In the other REM's, however, the plasmon resonance is sensibly stronger than that of the rest of the spectrum, and cannot be attributed to spurious effects. Moreover, the shape of the intensity curves becomes broader and the maxima fall at an energy ~ 10 eV higher than those observed for the f - f cross section. An increase in the plasmon intensity when E_p is close to the binding energy of the $5p$ or $4d$ core levels has been observed by Stenborg and Bauer in Sm and Yb.³⁴ We suggest that the plasmon excitation mechanism sketched in Fig. 10(c)—i.e., plasmon creation induced by the capture of the primary electron into an f state—should be particularly effective in all the REM's because of the localization of the f electrons, and should give a contribution not much smaller than that of the normal process sketched in Fig. 10(d). Both processes have a resonant counterpart, shown in Figs. 10(e) and

10(f). In process (f) the plasmon is an "intrinsic plasmon" excited by the switching on of the d core hole when the primary electron at E_p falls into an f state. The creation of this intrinsic plasmon when the excitation energy is only slightly above the core threshold, however, should be detectable also in the optical-absorption spectra. On the contrary, no plasmon satellite is found in the published optical data.⁴⁰ For this reason we suggest that the process that contributes the most to the plasmon resonance is that given by Fig. 10(e), i.e., the increase in the " f -plasmon" excitation probability due to the resonance enhancement of the cross section for the capture of the primary electron into an f state when $E_p \sim E_{4d}$.

The cross sections of the f - f and of the plasmon excitations in Gd show a maximum at about 120 eV followed by a monotonic descent with the exception of the resonance region. A similar maximum was found in Eu by Bauer and Kolaczkiwicz.¹³ In this metal the intensity of the f - f transitions grows monotonically from 20 to 100 eV. The initial increase and the maximum at ~ 100 eV can be explained if we assume that the primary electron has the highest probability to decay into an f state when it is in a g state. This holds if the selection rules for the emission of the virtual photon are similar to those for a real photon. The partial density of states with $l=4$ has a maximum at about 70 eV above the mean potential for a free electron in a sphere with radius equal to the Wigner-Seitz radius of Gd.⁴¹ Accordingly, the photoemission cross section of the f levels in Gd (which is mainly due to $4f \rightarrow 4g$ transitions) also has a maximum at about 100 eV.⁴² The decrease of the f - f cross sections at high E_p can be easily understood in terms of the energy dependence of the exchange mechanism.⁴³ This behavior is common to all the investigated REM's.

IV. CONCLUSIONS

We have shown that the energy-loss spectra of the rare-earth metals are characterized by sharp peaks due to exchange-excited dipole-forbidden f - f transitions. This attribution is supported by the comparison between the EEL spectra of the metal with n f electrons and the optical-absorption spectra of the corresponding trivalent ion and the BIS (x-ray photoemission spectrum) of the metal with $n-1$ f electrons ($n+1$ f electrons). The f - f peaks are particularly evident for primary energies close to the $4d$ binding energy, but in Sm and Gd they are strong also for E_p much smaller than E_{4d} . The core level related resonance of the f - f multiplets fits nicely into the picture of an electron-exchange excitation of the f - f transitions. An enhancement of the intensity of the plasmon peak when E_p reaches the $4d$ core threshold—particularly evident for the heavy rare-earth metals—is also found. In our opinion this effect points to a scattering mechanism in which the plasmon is excited by the temporary capture of a primary electron into an f state.

On the basis of our results, we predict that exchange-excited sharp multiplets of dipole-forbidden transitions should be detectable also in other systems with unfilled localized levels, such as the transition-metal oxides.

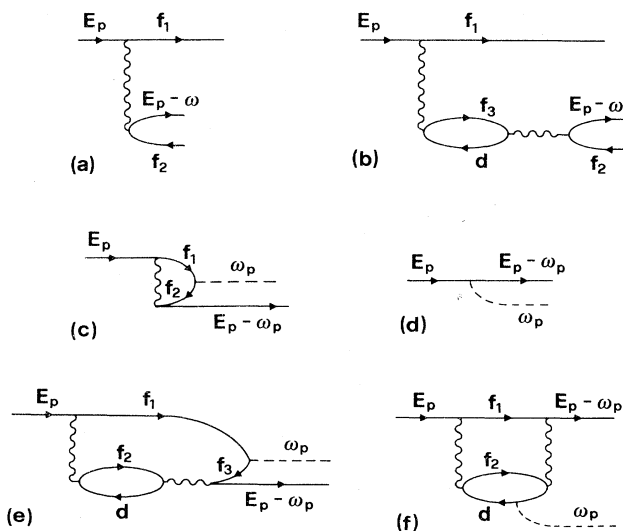


FIG. 10. Schematic diagrams describing the electron exchange excitation mechanism of (a) the f - f transitions (b) its resonant counterpart. (c) Plasmon shake-up process related to the temporary capture of a primary electron into an f state and (d) normal plasmon excitation process. The resonant counterparts of processes (c) and (d) are shown in (e) and (f).

ACKNOWLEDGMENTS

We are deeply indebted to E. Tosatti for the many helpful discussions and suggestions which, in particular, led to the clarification of the possible mechanisms of the

resonance processes. We thank R. Rosei for continuous encouragement. We acknowledge financial support by the Area per la Ricerca Scientifica e Tecnologica of Trieste.

- ¹See, for instance, H. S. W. Massey and E. H. S. Burhop, *Electronic and Ionic Impact Phenomena* (Oxford University Press, London, 1952), p. 141 ff and p. 156 ff; a review paper is G. F. Hanne, *Phys. Rep.* **95**, 95 (1983).
- ²See, for instance, A. Kuppermann, W. M. Flicker, and O. A. Mosher, *Chem. Rev.* **79**, 77 (1979), and references therein.
- ³C. J. Powell and N. E. Erickson, *Phys. Rev. Lett.* **51**, 61 (1983); D. Mauri, R. Allenspach, and M. Landoldt, *ibid.* **52**, 152 (1984).
- ⁴F. P. Netzer, G. Strasser, and J. A. D. Matthew, *Phys. Rev. Lett.* **51**, 211 (1983); J. A. D. Matthew, G. Strasser, and F. P. Netzer, *Phys. Rev. B* **27**, 5839 (1983); G. Strasser, G. Rosina, J. A. D. Matthew, and F. P. Netzer, *J. Phys. F* **15**, 739 (1985).
- ⁵H. Hopster, R. Raue, and R. Clauber, *Phys. Rev. Lett.* **53**, 695 (1984).
- ⁶J. Kirschner, D. Rebenstorff, and H. Ibach, *Phys. Rev. Lett.* **53**, 698 (1984).
- ⁷J. Kirschner, *Phys. Rev. Lett.* **55**, 973 (1985); J. Kirschner and S. Suga, *Surf. Sci.* **178**, 327 (1986); D. Venus and J. Kirschner, *Phys. Rev. B* **37**, 2199 (1988).
- ⁸Y. U. Idzerda, D. M. Lind, D. A. Papaconstantopoulos, G. A. Prinz, B. T. Jonker, and J. J. Krebs, *Phys. Rev. Lett.* **61**, 1222 (1988).
- ⁹J. Glazer and E. Tosatti, *Solid State Commun.* **52**, 905 (1984).
- ¹⁰S. Modesti, F. Della Valle, R. Rosei, E. Tosatti, and J. Glazer, *Phys. Rev. B* **31**, 5471 (1985).
- ¹¹S. Modesti, F. Della Valle, C. J. Bocchetta, E. Tosatti, and G. Paolucci, *Phys. Rev. B* **36**, 4503 (1987).
- ¹²S. Modesti, G. Paolucci, and E. Tosatti, *Phys. Rev. Lett.* **55**, 2995 (1985); S. Modesti, F. Della Valle, and G. Paolucci, *Phys. Scr.* **T19**, 419 (1987).
- ¹³E. Bauer and J. Kolaczkiwicz, *Phys. Status Solidi B* **131**, 699 (1985).
- ¹⁴Calibration of the oxygen coverage was obtained measuring differing Auger spectra as a function of oxygen exposure assuming a unitary sticking coefficient. Fo Gd, 0.02 monolayers corresponds to a ratio of the oxygen peak to the 835 eV Gd peak smaller than 0.03. The spectra were measured with constant $\Delta E/E$ and 5-V modulation.
- ¹⁵G. K. Wertheim and G. Crecelius, *Phys. Rev. Lett.* **40**, 813 (1978).
- ¹⁶J. K. Lang and Y. Baer, *Solid State Commun.* **31**, 945 (1979).
- ¹⁷W. T. Carnall, P. R. Fields, and K. Rajnak, *J. Chem. Phys.* **49**, 4412 (1968).
- ¹⁸J. K. Lang, Y. Baer, and P. A. Cox, *Phys. Rev. Lett.* **42**, 74 (1979); *J. Phys. F* **11**, 121 (1981).
- ¹⁹Y. V. Knyazev and M. N. Noskov, *Fiz. Met. Metalloved.* **30**, 214 (1970) [*Phys. Met. Metallogr. (USSR)* **30**, 230 (1970)].
- ²⁰A. Quemarais, B. Loisel, G. Jezequel, J. Thomas, and J. C. Lemonnier, *J. Phys. F* **11**, 293 (1981).
- ²¹C. Colliex, M. Gasgnier, and P. Trebbia, *J. Phys. (Paris)* **37**, 397 (1976).
- ²²J. H. Weaver, C. Krafska, D. W. Lynch, and E. E. Koch, *Optical Properties of Metals Pt. II*, Physics Data 18-2 (Fachinformationszentrum, Energie Physik Mathematik GmbH, Karlsruhe, 1981).
- ²³F. H. Combley, E. A. Stewardson, and J. E. Wilson, *J. Phys. B* **1**, 120 (1968); W. C. Lang, B. D. Padalia, L. M. Watson, and D. J. Fabian, *J. Electron Spectrosc. Relat. Phenom.* **7**, 357 (1975); B. D. Padalia, W. C. Lang, P. R. Norris, L. M. Watson, and D. J. Fabian, *Proc. R. Soc. London, Ser. A* **354**, 269 (1977); L. I. Johansson, J. W. Allen, I. Lindau, M. H. Hecht, and S. B. M. Hagtröm, *Phys. Rev. B* **21**, 1408 (1980).
- ²⁴F. P. Netzer, G. Strasser, G. Rosina, and J. A. D. Matthew, *Surf. Sci.* **152/153**, 757 (1985).
- ²⁵Y. Baer and G. Bush, *J. Electron Spectrosc. Relat. Phenom.* **5**, 611 (1974).
- ²⁶F. Gerken, *J. Phys. F* **13**, 703 (1983).
- ²⁷H. H. Caspers, H. E. Rast, and R. A. Buchanan, *J. Chem. Phys.* **43**, 2124 (1965).
- ²⁸H. M. Crosswhite, H. Crosswhite, F. W. Kaseta, and R. Sarup, *J. Chem. Phys.* **64**, 1981 (1976).
- ²⁹It is also worth noting that the photoemission spectrum of Nd of A. Platau, A. Callenäs, and S.-E. Karlsson, *Solid State Commun.* **37**, 829 (1981) does not show with the same evidence the ³P states of the f^2 configuration that appear in the EEL spectra of Pr at $\omega=2.6$ eV.
- ³⁰J. W. Allen, L. I. Johansson, I. Lindau, and S. B. Hagström, *Phys. Rev. B* **21**, 1335 (1980).
- ³¹J. Onsgaard and I. Chorkendorff, *Phys. Rev. B* **33**, 3503 (1986).
- ³²E. Bertel, G. Strasser, F. P. Netzer, and J. A. D. Matthew, *Surf. Sci.* **118**, 387 (1982).
- ³³J. G. Endriz and W. E. Spicer, *Phys. Rev. B* **2**, 1466 (1970).
- ³⁴A. Stenborg and E. Bauer, *Solid State Commun.* **66**, 561 (1988).
- ³⁵J. Onsgaard, I. Chorkendorff, and O. Sørensen, *Phys. Scr.* **T4**, 169 (1983).
- ³⁶H. M. Crosswhite and G. H. Dieke, *J. Chem. Phys.* **35**, 1535 (1961).
- ³⁷D. Mills, *Surf. Sci.* **48**, 59 (1975); H. Ibach and D. Mills, *Electron Energy Loss Spectroscopy and Surface Vibrations* (Academic, New York, 1982).
- ³⁸T. M. Zimkina, V. A. Fomichev, S. A. Gribovskii, and I. I. Zhukova, *Fiz. Tverd. Tela* **9**, 1447 (1967) [*Sov. Phys.—Solid State* **9**, 1128 (1967)]; V. A. Fomichev, T. M. Zimkina, S. A. Gribovskii, and I. I. Zhukova, *ibid.* **9**, 1490 (1967) [**9**, 1163 (1967)]; S. A. Gribovskii and T. M. Zimkina, *ibid.* **15**, 300 (1973) [**15**, 217 (1973)].
- ³⁹J. Sugar, *Phys. Rev. B* **5**, 1785 (1972).
- ⁴⁰R. Haensel, P. Rabe, and B. Sonntag, *Solid State Commun.* **8**, 1845 (1970); T. M. Zimkina, V. A. Fomichev, and S. A. Gribovskii, *Fiz. Tverd. Tela* **15**, 1629 (1973) [*Sov. Phys.—Solid State* **15**, 1097 (1973)]; V. A. Fomichev, S. A. Gribovskii, and T. M. Zimkina, *ibid.* **15**, 2817 (1973) [**15**, 1880 (1974)]; C. G. Olson and D. W. Lynch, *J. Opt. Soc. Am.* **72**, 88 (1982).
- ⁴¹J. E. Müller and J. W. Wilkins, *Phys. Rev. B* **29**, 4331 (1984).
- ⁴²J. J. Yeh and I. Lindau, *At. Data Nucl. Data Tables* **32**, 1 (1985).
- ⁴³C. J. Bocchetta, E. Tosatti, and S. Yin, *Z. Phys. B* **67**, 89 (1987).